# Electronic properties and electron dynamics of the Si(001)(2×1) surface with C-defects

S. Tanaka and K. Tanimura
*The Institute of the Industrial and Scientific Research, Osaka University, 567-0047 Mihogaoka, Ibaraki, Osaka, Japan*
(Received 8 June 2006; revised manuscript received 13 September 2007; published 23 May 2008)

Both the time-resolved two-photon photoelectron spectroscopy and scanning tunneling microscopy are utilized for investigating the role of the C-defects in the electronic property and dynamics of the *p*-type Si(001)(2×1) surface. It is found that the C-defect causes Fermi-level pinning when its density is more than 0.05 monolayer. The change in the inverse of the product of the bulk-to-surface electron transition rate $S$ and in the extinction lifetime $\tau$ of the surface excited electron is examined as a function of the C-defect density, and it was found that the change doubles when the C-defect density increases from 0 to 0.1 monolayer on the surface. This indicates that the C-defect plays an important (but limited) role in the surface carrier dynamics of Si(001).

DOI: 10.1103/PhysRevB.77.195323 PACS number(s): 78.47.−p, 73.25.+i, 73.50.Gr

## I. INTRODUCTION

The atomic configuration and electronic properties of the defects on semiconductor surfaces have been studied extensively since they strongly influence the electronic properties, surface morphology, absorption, etc, of the surface in many cases.[1–7] A typical example is defects on the Si(001)(2×1) surface, which is one of the most extensively studied because of its technological importance for device fabrication. The "ideal" Si(001)(2×1) surface consists of the buckled dimers at room temperature. However, it is known that this surface usually contains defects, which may play crucial roles in many aspects. In the pioneering work of Hamers and Koehler[1] using scanning tunneling microscopy (STM), the defects on Si(001) are classified into three groups, termed as "A," "B," and "C" types. The A- and B-defects are single and double dimer vacancies, respectively. The local electronic structures of A- and B-defects are semiconducting as well as a normal dimer according to scanning tunneling spectroscopy (STS).[1,2] Meanwhile, the C-defect shows a metallic feature in the local electronic state, and is ascribed to the origin of the Fermi-level pinning on this surface.[1–3] The C-defect is, therefore, of particular interest and has been extensively studied thus far. The C-defect appears as two protrusions in the STM image, whose appearance depends on the sample bias, i.e., bright at positive sample bias (empty-state image) or dark at negative sample bias (filled-state image) on one half and depressions on the other half of two adjacent dimers in a row.[1–3] The origin and atomic structure of the C-defect have been debated since the work of Hamers and Koehler. Chander *et al.*[4] argued that C-defect features are derived from the molecularly adsorbed water molecules which are contained in ambient pressure. Recently, Nishizawa *et al.*[5] proposed that the C-defect is caused by the dissociative adsorption of the water molecule. This concept was confirmed by Hossain *et al.*[6] and Okano and Oshiyama,[7] although a detailed configuration of the C-defect was corrected. In their new model, the H and OH of dissociated water are adsorbed on the same side of the adjacent dimers, and the metallic electronic state of the C-defect is due to the remaining dangling bond of the decorated dimers, and this causes the bright spot in the STM images of the unoccupied states. In spite of these microscopic works, the relation between the macroscopic electronic properties of the Si(001) surface as a function of the C-defect density is still unclear.

The electron dynamics on the Si(001) surface, meanwhile, attracts much attention, and several studies were carried out on the "clean" Si(001)(2×1) surface.[8–18] These studies revealed that several processes, i.e., the bulk-to-surface electron transition, electron extinction from the surface states, diffusion of the electron within the bulk states into deeper bulk, etc., play important roles in the surface carrier dynamics of the Si(001)(2×1) surface. However, as noted before, the (2×1) surface usually contains a small percentage of defects when it is prepared in a standard condition. It is probable that the surface defects play an important role in the electron dynamics of the Si(001) surface. Therefore, it is highly desirable to elucidate the role of the defects in the carrier dynamics of the Si(001) surface.[18] However, to our knowledge, there is no study in which the role of the defects in the electron dynamics is examined quantitatively, i.e., under the conditions where the number and types of the defects are well defined.

The main aim of this paper is to elucidate the role of the C-defect in the electronic properties and dynamics of the Si(001) surface by the combined measurements of STM and time-resolved two-photon photoelectron (TR-2PPE) spectroscopy.

## II. EXPERIMENTS

The experiments were carried out in an UHV system consisting of three UHV chambers. The main chamber is equipped with an electron analyzer for 2PPE, and another one with a STM. A Si(001) wafer (B-doped, 10 Ω cm) is installed within a sample holder originally constructed for the STM, and can be transferred *in situ* between these two chambers through the other UHV chamber which is used for the preparation and exchange of the sample and the STM tip. Base pressures of the STM chamber, preparation chamber, and 2PPE chamber were $3\times10^{-11}$, $4\times10^{-11}$, and $5\times10^{-11}$ Torr, respectively. The 2PPE chamber was equipped with a shroud cooled with liquid nitrogen for reducing the pressure.

 

The laser pulses of 754 nm (1.64 eV) with 150 fs width, generated by a mode-locked Ti:sapphire laser at 76 MHz repetition rate, were used as pump pulses, and the frequency-tripled pulses (4.91 eV) with the temporal width of 320 fs, generated with two 0.5-mm thick BBO crystals, were used as probe pulses. These pulses with a preset time delay ($\Delta t$) were aligned coaxially, and were focused on surfaces at about 0.2 mm in diameter (for the pump beam) with the incident angle of 45° from the surface normal. The probe and pump pulses were p-polarized. The power of the probe pulses was about 10 $\mu J/cm^2$, and that of the probe pulses was about 10 $nJ/cm^2$. Electrons emitted along the surface normal were analyzed with the hemispherical analyzer equipped with 16-channel detectors, each of which monitors the intensity of the electron of a different kinetic energy separated by 0.014 eV. We used two modes for the 2PPE measurement. In one mode, here we call it as an E-scan mode, the center energy of the electron analyzer was scanned at a fixed $\Delta t$ in a way that conventional photoelectron spectroscopy is measured. In this mode, the signals from each channel of detectors were added after adjusting the energy. In the other mode, which we call a T-scan mode, the photoelectron intensities at 16-channel detectors are measured simultaneously at several fixed center energies as a function of $\Delta t$. Efficiencies of the 16-channel detectors are calibrated by comparing the energy-scan spectra obtained by the respective detectors.

The sample was cleaned by resistive heating at about 1100 °C for more than 10 s in the 2PPE chamber with a pressure below $8\times10^{-11}$ Torr at maximum, and then slowly ($<4$ K/s) cooled to room temperature. STM images were taken with a W tip. For the filled- (empty-) state image, sample voltage of +2.0 (−1.8) V and the tunneling current of 0.25 nA were used. We found that the number of the defects, not only the C-defects but also A- and B-defects, was strongly dependent on the vacuum condition during the heating and also on the history of the sample.

## III. RESULTS

### A. Scanning tunneling microscopy observation

Figure 1 shows the densities of the three types of defects observed in the STM images of Si(001) as a function of the elapsed time after the cleaning. The sample was heated at the 2PPE chamber, and then transferred into the STM chamber in 30 min. The position of the tip on the sample was frequently moved in order to make an average over the area of the sample. A number of the C-defects were counted in the empty-state image, and those of the A- and B-defects were counted in the filled-state image by comparing two images of the same area. Note that we took the number of dimers as a unit of the defects, i.e., one A-defect counts as one, whereas one B- and one C-defect count as two, respectively, and then divided by the total number of the dimers including the missing dimers in the counted area. It is evident that the number of the C-defects linearly increases with the elapsed time after the cleaning, while those of the A-and B-defects stay nearly constant. This confirms the recent report by Nishizawa *et al.*,[5] and is consistent with the model that the C-defect is due to the adsorption of the water molecule in ambient pressure,

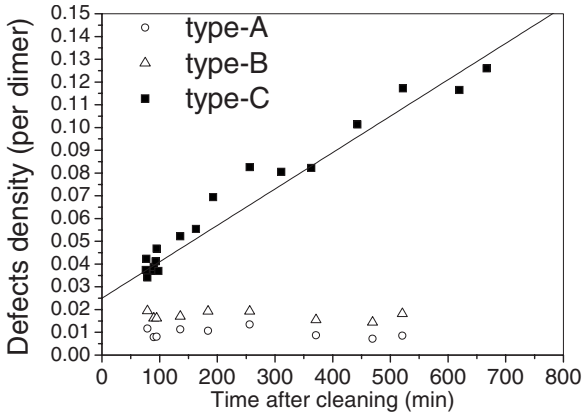


FIG. 1. Defect density examined by using STM as a function of the elapsed time after the cleaning. Open circles, open triangles, and solid squares represent the densities of A-, B-, and C-defects, respectively. The solid line is a guide for the eye.

while the A- and B-defects are intrinsic ones to the sample. The estimated coverage of the C-defects just after the cleaning is not zero, probably due to the adsorption during the heating procedure and/or the sample transfer. Note that the surface used in the experiment for Fig. 1 was rather defect-rich; the total density of the missing dimer is about 3% just after the cleaning. We made a similar measurement for a less defective surface (total density of missing dimer due to A- and B-defects was less than 1%), and found that the number of the C-defects increases with elapsed time in a similar slope, but the estimated initial C-defect density was almost zero in this case.

### B. 2PPE spectroscopy

All the 2PPE measurements were carried out for the Si(001)$(2\times1)$ surface on which the density of the missing dimer is less than 1%. Figure 2 shows the 2PPE spectra of the Si(001) surface with typical C-defect densities given in monolayer (ML) of the decorated dimer, as a result of the continuous measurements in the 2PPE chamber. The elapsed time (in the 2PPE chamber) after cleaning was 40 min [Fig. 2(a)], 300 min [Fig. 2(b)], and 580 min [Fig. 2(c)], respectively. The C-defect densities as a function of the elapsed time were estimated by careful comparisons of 2PPE spectra with the STM images taken after the successive transfer of the sample between two chambers. The error of the calibration was estimated as ±0.004 ML at the C-defects of 0.06ML. Three solid lines represent the spectra taken at the pump-probe time difference ($\Delta t$) of 6, 0, and −6 ps, respectively, from top to bottom. Dashed lines show 30-times magnified curves of the spectra at $\Delta t=6$ ps. Dotted lines are the spectra taken only with the probe pulse (without the pump pulses). The scale of the horizontal axis in Fig. 2 shows the intermediate energy (of the unoccupied state) with respect to the conduction band minimum (CBM). This was derived from the Fermi level, which is located at 0.88 eV (calculated from the dopant density of the sample) below the CBM, both at the surface and in the bulk, since the flatband condition is considered to be achieved for the clean Si(001)$(2\times1)$

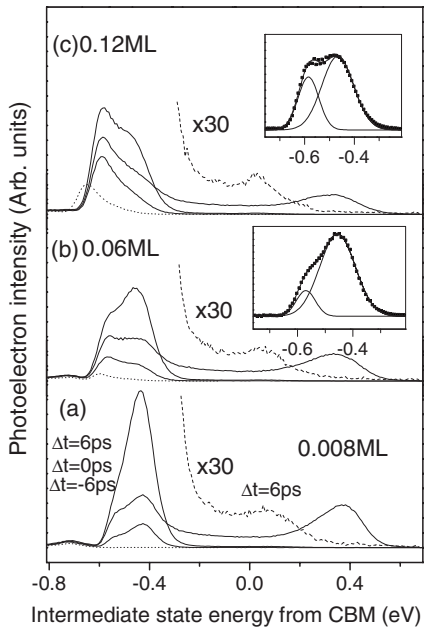


FIG. 2. Two-photon photoelectron spectra of the Si(001) surface which contains C-defect of (a) 0.008 ML, (b) 0.06 ML, and (c) 0.12 ML. Three solid lines represent the spectra taken at the pump-probe time difference ($\Delta t$) of 6, 0, and −6 ps, respectively, from top to bottom. Dashed lines show 30-times magnified curves of the spectra at $\Delta t=6$ ps. Dotted lines are the spectra taken only with the probe pulse (without the pump pulses). In the insets, the spectra of $\Delta t=6$ ps subtracted from the spectra of $\Delta t=-6$ ps (dots) and fitting curves assuming the Gaussian shape (solid lines). See the text for further details.

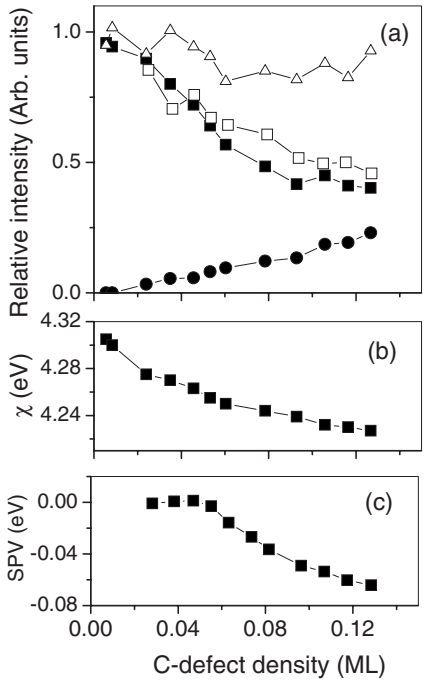


FIG. 3. (a) The relative intensities of the peaks at ~−0.44 eV ($\Delta t=6$ ps, filled square), ~0.38 eV ($\Delta t=0$ ps, open square), ~0.06 eV ($\Delta t=6$ ps, open triangles), and ~−0.6 eV ($\Delta t=6$ ps, filled circles) in the 2PPE spectra as a function of the C-defect density. Before evaluating, the spectra are subtracted by the spectra at $\Delta t=-6$ ps. See the text for further details. (b) The electron affinity $\chi$, measured with the onset energy of the pump-probe spectra, as a function of the C-defects. (c) Surface photovoltage, measured with the shift of the onset energy of the probe-only spectra from that of the pump-probe spectra. See the text for further details.

surface.[13–17] The Fermi level of the spectrometer was determined by measuring the 2PPE spectrum of the Ta holder.

The spectra of the surface which contains a small amount of the C-defects [Fig. 2(a)] are similar to the one in previous studies,[13–17] and peaks can be interpreted as follows. The peaks at ~−0.44 eV are ascribed to the unoccupied $D_{\text{down}}$ of the $(2\times1)$ dimer. The interpretation of the peak at ~0.38 eV is not straightforward. It had been interpreted as a two-photon coherent photoelectron emission from the occupied $D_{\text{up}}$ state.[13,14] Afterwards, this peak was reinterpreted to be the $n=1$ intermediate (imaginary) state close to the vacuum level by Weinelt *et al.*,[16] when the UV-photon energy is approximately 4.77 eV. Whatever this peak is, it is observed only when the pump and probe pulses are temporarily overlapped, and we will not discuss this further as it is beyond the scope of this paper. Small peaks at ~0.06 eV observed in the magnified curves at $\Delta t=6$ ps have been ascribed to the emission from the bulk conduction band.[9,17] The small structure at ~−0.55 eV has been observed in previous studies as well,[14–17] and is attributed to the emission from the unoccupied defect state, which is consistent with the results shown below. The origin of the very small peak at −0.7 eV, which was not reproducible and should not be ascribed either to the clean Si(001)$(2\times1)$ surface or to the C-defect, is not known until now.

The energy diagram of the Si surface with C-defects of 0.008 ML is schematically shown as solid lines in Fig. 4(a). Note that the band is flat due to the surface photovoltage effect. Therefore, the energies can be referred to the Fermi level in the bulk and to the CBM as well. The kinetic energy of the electron is determined with respect to the Fermi level of the analyzer, which is aligned to that of the sample, as shown in the right hand side of Fig. 3(a). The errors in the energy level are about ±0.05 eV.

As the density of the C-defects increases [Figs. 2(b) and 2(c)], the 2PPE spectra show gradual changes. We will focus on three characteristic changes. The first is the change in the peak intensity. The $D_{\text{down}}$ and ~−0.38 eV peaks are decreased in intensity without any apparent change in energy (<0.02 eV), while the peak at about −0.6 eV is increased in intensity and decreased in energy when the C-defect density increases. The peak at about −0.6 eV is ascribed to the unoccupied state originating from the C-defect. The constant position of the $D_{\text{down}}$ and the bulk peaks indicates that the flatband condition is still achieved for the surface with the C-defects of <0.12 ML, when illuminated by the pump and probe pulses. The bulk peak is also unchanged in energy, and intensity decrease with increasing C-defect density is smaller than that of the $D_{\text{down}}$. Figure 3(a) shows relative intensities of the $D_{\text{down}}$ peak at $\Delta t=6$ ps (filled square), the ~0.38 eV peak at $\Delta t=0$ ps (open square), and the peak of the bulk conduction band at $\Delta t=6$ ps (open triangle), after the normalization such that it is 1 at zero C-defect density. The intensity of the defect peak at $\Delta t=6$ ps is also shown in the

same scale for the $D_{down}$ peak (filled circle). In order to exclude the effects of the preceding pump pulse as well as the photoemission due only to the probe pulse, all the spectra of $\Delta t=6$ ps and $\Delta t=0$ ps were subtracted with the spectrum at $\Delta t=-6$ ps before these evaluations. The intensities for the bulk conduction band and the ~0.38 eV peaks were obtained by the area intensities in the range from 0 to +0.12 eV, and those from 0.14 to 0.54 eV, respectively. For evaluating the intensities of the $D_{down}$ and C-defect peaks, a fitting calculation was carried out using two Gaussian peaks. Examples of the results of the fitting are shown in the inset of Figs. 2(b) and 2(c). Generally speaking, the correlation between the calculated curve and the data was fairly high for the $D_{down}$ peak, but not so high at the C-defect peak when the C-defect density was increased, although the error was not significant in estimating the peak area intensity.

Reductions of the ~0.38 eV and $D_{down}$ peak intensities with increasing elapsed time after the cleaning were also observed in the previous study.[14] However, the half-value period at the previous study was about one-fifth of the present one. This change may be due to a reduced partial pressure of water, which is caused by a liquid nitrogen reservoir in the present study. This supports the interpretation in which the C-defect is due to water adsorption.

The second feature is a shift in the lower onset energy of the 2PPE spectra (taken with pump and probe pulses) with increasing C-defect density. The shift is independent of $\Delta t$, and is ascribed to the decrease in the work function. In the case of the semiconductor surface, the ionization energy $\xi$ [the energy of the vacuum level with respect to the valence band maximum (VBM)] or the electron affinity $\chi$ (the energy of the vacuum level with respect to the CBM) is often used instead of the work function (the energy of the vacuum level with respect to the Fermi level), since the position of the Fermi level can be changed within the band gap depending on the dopant, temperature, etc. Here, we take the electron affinity $\chi$ since we now take the conduction band minimum as the energy reference. Figure 3(b) plots the electron affinity $\chi$, which was derived as $\chi=h\nu(\text{probe})+E_{threshold}$, where $h\nu$(probe) is the photon energy of the probe pulse (4.91 eV) and $E_{threshold}$ is the lower onset energy of the spectra with respect to the CBM. We obtained 4.31 eV as the electron affinity $\chi$ and 5.42 eV as the ionization energy $\xi$ (since the band gap of Si is 1.11 eV) for the clean Si(001) surface. These are similar to the one previously reported.[13] The electron affinity $\chi$ decreases with increasing C-defect density as shown in Fig. 3(b).

The energy diagram of the Si surface with C-defects of 0.12 ML (dotted lines) is schematically shown in Fig. 4(a). The lower onset energy in the spectra ($E_{threshold}$) corresponds to the level from which the energy of the electron excited with the probe photons reaches the vacuum level of the sample.

The third feature is a change of the photoelectron emission due only to the probe pulse (dotted line). With the increasing C-defect density, this emission shows not only an increase in intensity, but also a shift in energy. This emission contains small peaks whose relative energies are in agreement, with respect to the lower onset, with those of the C-defect, $D_{down}$, and bulk peaks in the spectra with pump and probe pulses. Therefore, this emission is ascribed to the photoelectron emission from these (mainly C-defect) unoccupied states. Since the relative peak energies with respect to the lower-energy onset were similar to those taken with the pump and probe pulses, the energy shift cannot be ascribed to the changes in the work function nor the binding energies of individual state, but should be attributed to the shift in the reference level. It indicates that the flatband condition is not achieved (the band bending occurs) when the surface is illuminated only by the weak probe pulse. Figure 3(c) shows the difference in the onset energy between the pump-probe spectra and the probe-only spectra. It is almost zero when the C-defect density is smaller than 0.05 ML, and then decreased with increasing C-defect density. More details in relation to the origin of this shift will be discussed later.

Figure 5 shows temporal evolutions of the peak intensities of $D_{down}$ peak [Fig. 5(a)] and the peak of the bulk conduction

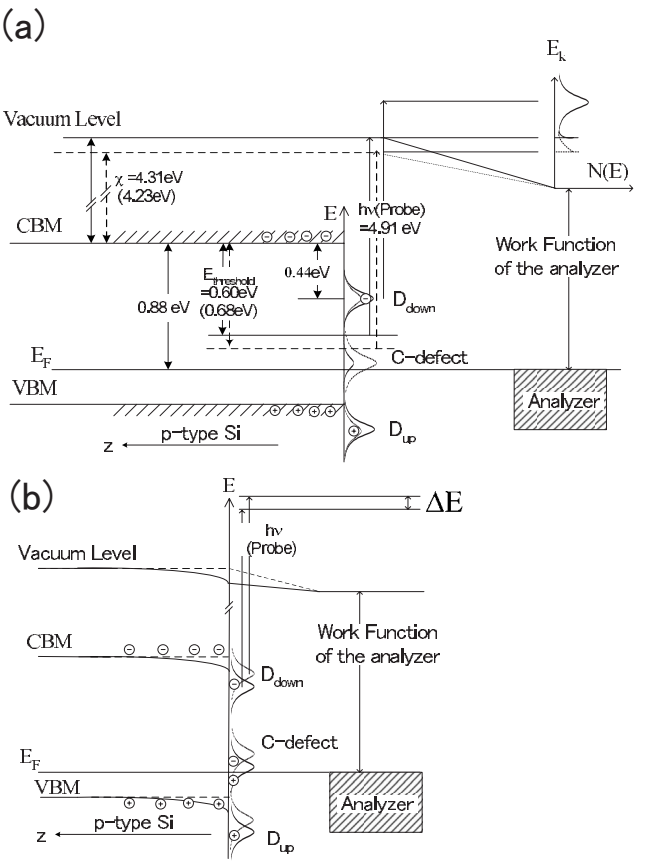


FIG. 4. (a) The schematic energy diagrams of the Si(001) surface covered with C-defect of 0.008 ML (solid lines) and 0.12 ML (dotted lines). The electron affinity and the $E_{threshold}$ for the surface with the C-defect of 0.008 ML (0.12 ML) are shown. The schematic picture of the electron spectrum obtained with the analyzer is also shown in the upper level at the right-hand side. (b) Schematic energy diagrams of the Si(001) surface with C-defects. When the surface is illuminated with a low intensity, the band bending remains (solid lines). On the other hand, when the surface is illuminated with a high intensity, the surface photovoltage effect makes the band flat. As a result, the spectrum is shifted in energy by $\Delta E$, even if the binding energies (with respect to the CBM) of the states remain constant. The errors in the energy levels are about $\pm 0.05$ eV.

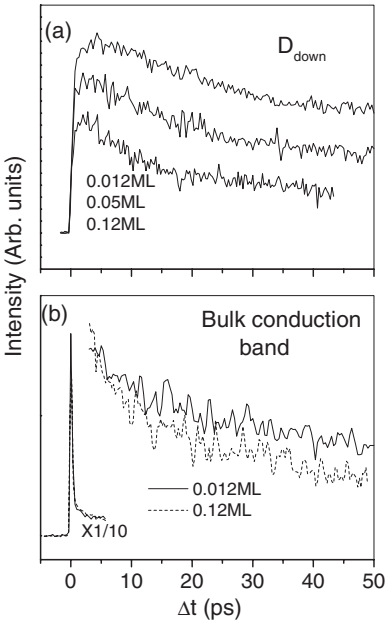


FIG. 5. Temporal evolutions of the intensity of (a) the $D_{\text{down}}$ and (b) the bulk conduction band for typical C-defect densities on Si(001). See the text for further details.

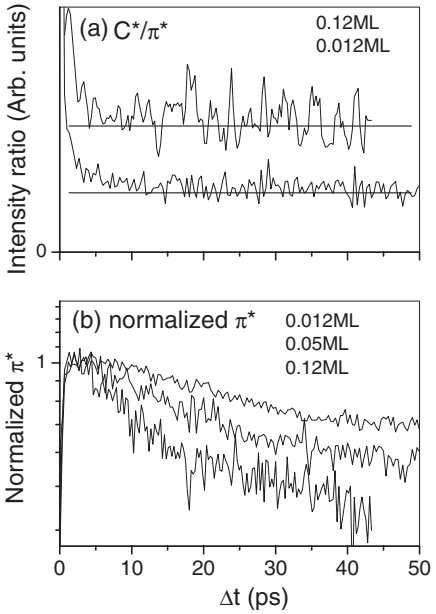


FIG. 6. (a) The intensity ratio of the peak of the bulk conduction band to the $D_{\text{down}}$ peak for typical C-defect densities on Si(001). The lines indicate constant values. (b) The normalized intensity of $\pi^*$ as a function of the pump-probe time delay for typical C-defect densities on Si(001).

band [Fig. 5(b)] for typical C-defect densities, obtained in the T-scan mode. The separation between the C-defect peak and the $D_{\text{down}}$ peak was made with the peak fitting using the two Gaussian curves in the range from −0.7 to 0.3 eV. In order to reduce the ambiguity, the peak width was fixed to the value obtained at calculation for the E-scan 2PPE spectra at $\Delta t=6$ ps. The result for the $D_{\text{down}}$ peak was similar to a simple summation within the region from −0.5 to −0.3 eV, except for reduced noises. For obtaining the intensity of the conduction band, the intensity was summed in the region from −0.06 to 0.14 eV. Large and sharp peaks at $\Delta t=0$ in Fig. 6(b) is ascribed predominantly to the emission due to the coherent two-photon absorption process of the electron at the overlapping occupied state, and the rather gradual decrease after $\Delta t > \sim 1$ ps is due to the decay of the bulk conduction band.

The intensities of these peaks represent the electron population at the respective unoccupied state, and they are referred to as $\pi^*$ and $C^*$, respectively, in the following. Note that $C^*$ represents the electron density of the region which is rather near the surface considering the penetration depth of the probe beam ($5.4\times10^{-7}$ cm). With increasing the C-defect density, the temporal evolution of these electron populations changes. In addition to an obvious decrease of $\pi^*$, we would like to point out two interesting features. First, for every C-defect density, intensities of these peaks are proportional to each other except for early $\Delta t$. This is demonstrated in Fig. 6(a), where the ratios of the $C^*$ to $\pi^*$ is plotted as a function of $\Delta t$ for typical C-defect densities. They are nearly constant at $\Delta t \sim 30$ ps, which means that $C^*$ and $\pi^*$ are proportional to each other. We confirmed that this proportionality continues with a similar ratio until (at least) $\Delta t = 300$ ps on the surface with C-defects of <0.12 ML. This proportionality had been observed on the clean Si(001) surface.[17] Second, the temporal evolution of normalized $\pi^*$ is changed as a function of the C-defect density. In Fig. 6(b), $\pi^*$ normalized to the intensity maximum is plotted in a logarithmic scale against $\Delta t$, for a typical C-defect density, which clearly demonstrates that a decrease of $\pi^*$ is more rapid at $\Delta t < \sim 30$ ps when the C-defect density is increased. This trend is also observed for the decay of $C^*$.

## IV. DISCUSSION

### A. Electronic properties of the Si(001)(2×1) surface with C-defects

As shown in Fig. 3(b), the electron affinity $\chi$ is decreased by 0.08 eV when the C-defect density is increased from 0 to 0.12 ML. Hamers and Koehler reported the decrease of the barrier height by 0.5 eV due to the C-defect,[1] while Ukraintsev *et al.*[2] and Fukumizu *et al.*[19] claimed that there is no evidence of the barrier height reduction at the C-defect site. The present result supports the results of Hamers and Koehler, and is also consistent with Ranke and Xing, who observed that water absorption of 2 L (1 L=$1\times10^{-6}$ Torr s) causes a decrease in ionization energy $\xi$ by 0.25 eV.[20]

Next, we will discuss the origin of the difference in the onset energy between the spectra taken with both pump and probe pulses and the spectra taken only with probe pulses when the C-defect density is more than 5%. As noted in the previous section, this difference is ascribed to the shift in the reference level. In the pump-probe experiments, the flatband condition is achieved via the surface photovoltage (SPV), in which the photogenerated electrons and holes are separated due to the electronic field associated with the band bending, and they compensate for the band bending in turn. According to the measurement combined with the 1.16-eV laser and the

synchrotron radiation,[21,22] the saturation fluence for the SPV on the clean Si(001) surface and that covered with $SiO_2$ layers is approximately 10 $\mu J/cm^2$. The fluence of the pump beam in the present condition ($\sim$10 $\mu J/cm^2$, 1.64 eV) is considered to be approximate to the saturation for the SPV. Therefore, the band is always nearly flat when the sample is illuminated with the pump beam. This situation is depicted schematically by the dotted lines in Fig. 4(b). On the other hand, the probe beam ($\sim$10 $nJ/cm^2$, 4.9 eV) is so weak that a small SPV is expected.[21,22] Therefore, when illuminated only with the probe beam, the band is considered to be bent. The electron at the unoccupied state is provided by the photoexcitation with the photons in the probe pulses. This situation is shown with the solid lines in Fig. 4(b). The observed energy in the spectra always refers to the Fermi level of the analyzer, and the spectrum will show apparent shift in energy when the amount of the band bending changes, which is indicated as $\Delta E$ in Fig. 4(b). Therefore, the onset-energy difference between the spectra taken with the pump and probe pulse and that only with the probe pulse should correlate with the band-bending energy at the surface. Although it is difficult to determine the value of the band bending precisely, it is possible to state that Fig. 3(c) indicates that the band bending on the Si(001) surface which contains C-defect of $<$0.05 ML is very small; in other words, the Fermi-level pining does not occur when C-defect density is less than 0.05 ML. Meanwhile, the Fermi-level pining occurs when C-defect density is more than 0.05 ML, and the energy of the band bending increases with the increase of the C-defect density (at least by $-$0.06 eV at C-defect of 0.12 ML). This band-bending energy shifts as a function of the C-defect density. This result clearly demonstrates in a macroscopic way that some amount ($>$0.05 ML) of C-defect can pin the Fermi level of the *p*-type Si(001) surface as predicted microscopically by using STM.[1]

According to Weinelt *et al.*,[16] the Fermi-level pinning of the *n*-type Si(001) surface occurs on the practically clean surface due to a small amount of defects, and this Fermi-level position with respect to CBM is $-$0.78 eV.[13] On the other hand, the Fermi level of the *p*-type Si(001) with C-defect of 0.12 ML is located at $\sim -$0.82 eV because SPV is 0.06 eV in the present study. These are in agreement with each other, and it is considered that it is the approximate position of the pinned Fermi level on the Si(001)$(2\times1)$ surface with the C-defects. According to the STS study,[1–3] the unoccupied state due to the C-defect is located just above the Fermi level both on the *p*- and *n*-type Si(001) surfaces. Therefore, the C-defect state is expected to be observed near $\sim -$0.82 eV (when C-defect density is 0.12 ML) with respect to CBM. However, this is located lower than the lower threshold energy in the preset condition as shown in Fig. 4(a). Therefore, we cannot expect that all of these states are detected in the present 2PPE spectra. Instead, what is observed as the C-defect "peak" in the 2PPE spectra only represents a higher-energy part of the unoccupied C-defect than the threshold energy. A shift in the peak energy as a function of the C-defect density is consistent with this interpretation. Furthermore, errors in the fitting procedure of the spectra assuming a symmetric Gaussian shape may support this. The fact that only part of the C-defect state is observed in the 2PPE spectra makes it difficult to evaluate the dynamics of the electron population within the C-defect state. This is the main reason why the temporal profile of the electron population at the defect state will not be discussed in the following section, although the dynamics of the localized state due to the adsorbed molecule is interesting.[22–24]

### B. Electron dynamics of the Si(001)$(2\times1)$ surface with C-defects

Figures 2(a), 3(a), and 6(a) show that the electron population at the $D_{down}$ state is decreased while the C-defect density increases. Figure 6(b) evidently shows that this is attributed not only to the reduction in the undecorated Si dimer of the $(2\times1)$ surface with increasing C-defect density, but also to the increase in the decay rate. The change in the electron dynamics due to the C-defects is also consistent with the fact that the decrease in the $D_{down}$ peak intensity at $\Delta t=6$ ps is larger than the absolute increase in the C-defect density [Fig. 3(a)].

In the previous study,[17] we measured the subnanosecond decay of $\pi^*$ and $C^*$ after the photoexcitation of the clean Si(001) surface. A prominent excitation-wavelength-dependent decay in subnanosecond temporal domain was observed for both $\pi^*$ and $C^*$, and they were proportional to each other at temporal regimes longer than 40 ps after the excitation. The results reveal a crucial role of the bulk-to-surface transition in the carrier dynamics of this surface, together with a short lifetime ($<$10 ps) of electrons at the $D_{down}$ state. In the previous work, a simple formula $d\pi^*/dt = SC^* - (\pi^*/\tau)$ was applied, since the excitation-density dependence was not observed at this temporal region. The first term on the right-hand side represents the electron flow from bulk to $D_{down}$ with a coefficient $S$, and the second term represents the extinction with a lifetime $\tau$. The decay of $C^*$ is governed by the diffusion into deeper bulk and the transfer into the surface state ("surface recombination"), as the intrinsic decay rate of the bulk photogenerated carriers is sufficiently slow for the present excitation densities (at most $10^{17}/cm^3$). If one approximates it under the condition that $(d\pi^*/dt)/\pi^*$ ($\sim$0.007 $ps^{-1}$ at $\Delta t>30$ ps) is much smaller than $1/\tau(>0.1)$,[16] it is reduced to $C^*/\pi^* \approx (S\tau)^{-1}$ (We took $C^*/\pi^*$ instead of $\pi^*/C^*$ since it practically gives a better signal to noise ratio.) Note that the above linear formula can no longer be applied to the temporal region of $\Delta t < \sim 30$ ps since the temporal evolutions of $\pi^*$ and $C^*$ significantly depended on the excitation intensity in this region.[13]

The present experimental results show that the proportion between $\pi^*$ and $C^*$ is nearly achieved at $\Delta t > \sim 30$ ps on the Si(001) surface with C-defects of $< \sim 0.12$ ML, and the ratio of $C^*$ to $\pi^*$ changes as a function of the C-defect density [Fig. 6(a)]. The C-defect state is located at $\sim$0.5 eV below the $D_{down}$ state; the electron transfer from the defect state is negligible at room temperature. Therefore, the above formula can be applied again, and $C^*/\pi^*$ is approximate to $(S\tau)^{-1}$ since when the C-defect density is increased, $(d\pi^*/dt)/\pi^*$ (0.0125 at 0.12 ML) is still much larger than $1/\tau$ ($> \sim 0.2$ at 0.12 ML; about twice the value at 0 ML as shown later).

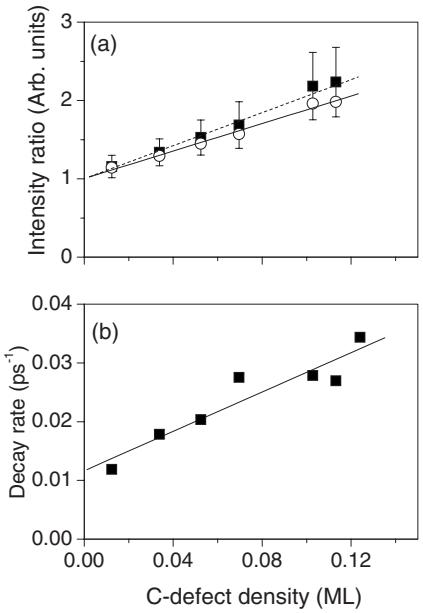


FIG. 7. (a) The intensity ratio of $C^*$ to $\pi^*$ averaged in the time domain of 40–45 ps after excitation (solid squares) and a line given by the least-squares fitting. The relative extinction rate (inverse of the lifetime) is also plotted (open circles). (b) Phenomenological decay rate of $\pi^*$ as a function of the C-defect density.

Note that the electron transfer from $D_{\mathrm{down}}$ to C-defect is included within the term of the extinction, and the decay of $C^*$ may be affected by the direct electron transfer to C-defect. In Fig. 7(a), the ratio of $C^*$ to $\pi^*$ averaged at $\Delta t$ of 40–45 ps, and normalized to the value at C-defect of 0 ML, is plotted as a function of the C-defect density (solid squares). Adding the C-defects of 0.1 ML on the Si(001) surface leads to a two-times increase in $(S\tau)^{-1}$. Therefore, it can be stated that the C-defect significantly affects the electron dynamics of the Si(001) surface, and, at the same time, also that this effect is limited for a practically clean surface covered with the C-defects of, say, 1% or 2%, since the increase in $(S\tau)^{-1}$ due to the C-defect is more or less 10% when the surface is covered with the C-defects of 0.01 ML.

Let us assume that the effect of the C-defect on the bulk-to-surface electron transfer is of a local nature, i.e., the C-defect density changes the electron flow coefficient $S$ as $S=S_0(1-x)$, where $S_0$ stands for the coefficient at a C-defect-free surface, and $x$ stands for the C-defect density. Then, the relative $\tau^{-1}$ can be derived, on this assumption, as a function of the C-defect density, and shown as open circles with a solid line in Fig. 7(a). It is still linearly increased with the C-defect density, and does not give a significant difference such that the above statement should be changed. This suggests that the C-defect works as a trapping state efficiently on the Si(0012)$(2\times1)$ surface. If the effect of the C-defect on the bulk-to-surface electron transition is somewhat delocalized, the slope (approximate to the probability of trapping at the C-defect site) will be more declined. We also evaluated the error as a result of the approximation due to the assumption of $1/\tau \gg (d\pi^*/dt)/\pi^*$ asuming $S=S_0(1-x)$, and found that this gives no significant difference (within 3%) in the estimation of $\tau^{-1}$ as a function of C-defect density when $\tau$ for the clean surface is shorter than 20 ps.

The above results indicate that the C-defect plays a somewhat minor role ($\sim$10%) in determining the lifetime of the electron at the $D_{\mathrm{down}}$ state of the practically clean Si(001) surface which contains the C-defect of, say, 1%, and other passes, e.g., trapping to other (A- and B-) defects, and/or the recombination with the holes at the bulk valence band, are predominant in the clean Si(001)$(2\times1)$ surface.

In the temporal domain of $\Delta t < \sim 30$ ps, where the above rate equations of first order can no longer be applied, the C-defect also affects significantly the electron dynamics as shown in Fig. 7(b). The phenomenological decay rate (inverse of the lifetime of the exponential decay) of $\pi^*$ derived in the region of $\Delta t < 25$ ps is shown in Fig. 6(b) as a function of the C-defect density. The decay rate increases with an increase of the C-defect density, and is three times larger when the C-defect density is about 0.1 ML compared with the case at 0 ML. This is consistent with the concept that the lifetime of $D_{\mathrm{down}}$ electron is shortened with an increase of the C-defect. However, the decay rate cannot simply be interpreted by certain physical properties. More work including the excitation-intensity dependence will be necessary for a further discussion.

Finally, we make a brief discussion about the components with an apparent long lifetime for the $D_{\mathrm{down}}$ and bulk states. In the 2PPE spectra, the peaks are observed not only when $\Delta t=0$ and 6 ps, but also when the $\Delta t=-6$ ps; in the case that the pump pulse does not reach the sample at the time when the probe pulse does, as shown in Figs. 2(a)–2(c). These are partly due to the preceding pump pulse, and indicate that there are long lifetime components in the decay of the electrons at these states, which are comparable to the pulse period (13.2 ns). These can be roughly estimated as

$$\frac{13.2}{\ln\left[1+\dfrac{I_6-I_{-6}-I_{3\omega}}{I_{-6}-I_{3\omega}}\right]},$$

where $I_6$, $I_{-6}$, and $I_{3\omega}$ denote the peak intensities when $\Delta t$ is 6 ps, when $\Delta t$ is $-6$ ps, and when only the probe pulse is injected, respectively. Note that this evaluation may give somewhat underestimated values, since faster components are ignored. We get the lifetimes of $\sim 7.2 \pm 1$ ns for both the $D_{\mathrm{down}}$ and the bulk states. These long lifetimes do not show a significant change when the C-defect density increases. This could be due to a number of reasons. The decay of the electron at the bulk conduction band is mainly due to the diffusion into deeper bulk in the early stage,[16] since the photogenerated carrier concentration is higher in the surface region than in the bulk region, and it becomes slower after the gradient of the carrier decreases enough. Then, in the temporal region when the carrier gradient is inverted (i.e., when it is lower in the near-surface region than the deeper bulk) due to the bulk-to-surface transition, the diffusion from the deeper bulk supplies the electron into the near-surface region and makes the decay slow. Since the population of the electron at the $D_{\mathrm{down}}$ state is dominated by the electron flow from the bulk conduction band,[16] a similar long lifetime is expected for the decay of the $\pi^*$. Note that the bulk electron decay does not depend on the (short) lifetime $\tau$ of the $D_{\mathrm{down}}$ elec-

tron, but on the surface-to-bulk transition coefficient $S$. If the effect of the C-defect on the bulk-to-surface electron transition is of a local nature, $S$ varies only by the about 10% when the C-defect increases to 0.1 ML. Therefore, a significant difference in the long lifetime is not expected.

## V. SUMMARY

TR-2PPE spectroscopy was utilized for investigating the electronic properties and electron dynamics of the Si(001)$(2\times1)$ surface on which the density of C-defect was examined with STM. It was found that the Fermi-level pinning occurs at $\sim-0.8$ eV with respect to CBM when C-defect density is more than 0.05 monolayer on the $p$-type Si(001)$(2\times1)$ surface. The electron dynamics of Si(001) is affected by the C-defect on the surface. A change in the inverse of the product of the bulk-to-surface electron transition rate $S$ and in the extinction lifetime $\tau$ for the surface electron is examined as a function of the C-defect density, and it was found that the change doubles when the C-defect density increases from 0 to 0.1 ML on the surface.

## ACKNOWLEDGMENT

This work was supported by a Grant-in Aid for Scientific Research from the Ministry of Education, Science, Sports, and Culture of Japan.

[1] R. J. Hamers and U. K. Koehler, J. Vac. Sci. Technol. A **7**, 2854 (1989).
[2] V. A. Ukraintsev, Z. Dohnálek, and J. T. Yates, Jr., Surf. Sci. **288**, 132 (1997).
[3] K. Hata, S. Ozawa, Y. Sainoo, K. Miyake, and H. Shigekawa, Surf. Sci. **447**, 156 (2000).
[4] M. Chander, Y. Z. Li, J. C. Patrin, and J. H. Weaver, Phys. Rev. B **48**, 2493 (1993).
[5] M. Nishizawa, T. Yasuda, S. Yamasaki, K. Miki, M. Shinohara, N. Kamakura, Y. Kimura, and M. Niwano, Phys. Rev. B **65**, 161302(R) (2002).
[6] M. Z. Hossain, Y. Yamashita, K. Mukai, and J. Yoshinobu, Phys. Rev. B **67**, 153307 (2003).
[7] S. Okano and A. Oshiyama, Surf. Sci. **554**, 272 (2004).
[8] R. Haight, Surf. Sci. Rep. **21**, 275 (1995).
[9] M. W. Rowe, H. Liu, G. P. Williams, Jr., and R. T. Williams, Phys. Rev. B **47**, 2048 (1993).
[10] J. R. Goldman and J. A. Prybyla, Phys. Rev. Lett. **72**, 1364 (1994).
[11] S. Jeong, H. Zacharias, and J. Bokor, Phys. Rev. B **54**, R17300 (1996).
[12] K. I. Shudo and T. Munakata, Phys. Rev. B **63**, 125324 (2001).
[13] C. Kentsch, M. Kutschera, M. Weinelt, Th. Fauster, and M. Rohlfing, Phys. Rev. B **65**, 035323 (2001).
[14] S. Tanaka and K. Tanimura, Surf. Sci. **529**, L251 (2003).
[15] M. Weinelt, M. Kutschera, T. Fauster, and M. Rohlfing, Phys. Rev. Lett. **92**, 126801 (2004).
[16] M. Weinelt, M. Kutschera, R. Schmidt, C. Orth, T. Fauster, and M. Rohlfing, Appl. Phys. A: Mater. Sci. Process. **80**, 995 (2005).
[17] S. Tanaka and K. Tanimura, Surf. Sci. **593**, 26 (2005).
[18] S. Jeong and J. Bokor, Phys. Rev. B **59**, 4943 (1999).
[19] H. Fukumizu, S. Kurokawa, and A. Sakai, Surf. Sci. **441**, 542 (1999).
[20] W. Ranke and Y. R. Xing, Phys. Rev. B **31**, 2246 (1985).
[21] W. Widdra, D. Bröcker, T. Gießel, I. V. Hertel, W. Krüger, A. Liero, F. Noack, V. Petrov, D. Pop, P. M. Schmidt, R. Weber, I. Will, and B. Winter, Surf. Sci. **543**, 87 (2003).
[22] D. Bröcker, T. Gießel, and W. Widdra, Chem. Phys. **299**, 247 (2004).
[23] K. Onda, B. Li, J. Zhao, K. D. Jordan, J. Yang, and H. Petek, Science **308**, 1154 (2005).
[24] B. Li, J. Zhao, K. Onda, K. D. Jordan, J. Yang, and H. Petek, Science **311**, 1436 (2006).